

# Chiral symmetry and resonances in QCD

M.F.M. LUTZ<sup>a,b</sup> and E.E. KOLOMEITSEV<sup>c</sup>

<sup>a</sup> *Gesellschaft für Schwerionenforschung (GSI)  
Postfach 110552, D-64220 Darmstadt, Germany*

<sup>b</sup> *Institut für Kernphysik, TU Darmstadt  
D-64289 Darmstadt, Germany*

<sup>c</sup> *The Niels Bohr Institute  
Blegdamsvej 17, DK-2100 Copenhagen, Denmark*

## Abstract

We study the formation of resonances in terms of the chiral SU(3) Lagrangian. At leading order parameter-free predictions are obtained for the scattering of Goldstone bosons off any hadron once we insist on approximate crossing symmetry of the unitarized scattering amplitude. A wealth of empirically established resonances are recovered and so far unseen resonances are predicted. Here we review in some detail the properties of light axial-vector mesons.

## 1 Introduction

A profound understanding of the nature of meson and baryon resonances is one of the outstanding issues of QCD. The discovery of meson and baryon resonance states with exotic quantum numbers turns this into a burning question deserving prime attention. The goal is to establish a systematic approach which is capable of describing and predicting the resonance spectrum of QCD quantitatively. In this context the authors' radical conjecture that meson and baryon resonances that do not belong to the large- $N_c$  ground state of QCD [1, 2, 3] should be generated in terms of coupled-channel dynamics strongly questions the quantitative applicability of the constituent-quark model to the resonance spectrum of QCD. In more explicit terms we expect that the resonance spectrum in the  $(u, d, s)$ -sector should be described in terms of the baryon-octet  $\frac{1}{2}^+$  and baryon-decuplet  $\frac{3}{2}^+$  fields together with the Goldstone boson  $0^-$  and vector meson  $1^-$  fields. In the large- $N_c$  and heavy-quark mass limit of QCD the latter baryon fields and also the latter meson fields have degenerate masses. If this change of paradigm is justified it requires to provide a systematic explanation of the many meson and baryon resonances established experimentally.

It is long known that the spectrum of light scalar mesons can be successfully reproduced in terms of coupled-channel dynamics as first pointed out by Törnqvist [4] and Van Beveren [5] in the 80s. In recent years this idea has been systematized by applying the chiral Lagrangian (see e.g. [6, 7]). Guided by the argument that in the heavy-quark mass limit one expects a degeneracy of the  $0^+$  and  $1^+$  meson spectra it is natural to expect a similar description of the axial-vector meson spectrum [3], to be reviewed in this talk. Even earlier in the 60s a series of works [8, 9, 10, 11, 12] predicted a wealth of s-wave baryon resonance generated by coupled-channel dynamics. Those works were based on a SU(3)-symmetric interaction Lagrangian that is closely related to the leading order chiral Lagrangian. For recent firm results on the spectrum of s- but also for the first time on d-wave baryon resonances based on the chiral Lagrangian see [13, 14]. In the latter works it was demonstrated that chiral SU(3) symmetry generates parameter-free the  $J^P = \frac{1}{2}^-$  and  $J^P = \frac{3}{2}^-$  baryon resonance spectrum. These results are important because they demonstrate that chiral coupled-channel theory is able to predict in which channels QCD forms resonance states.

The spectrum of axial-vector mesons is obtained by studying the scattering of Goldstone bosons off vector mesons using the leading order chiral Lagrangian. Our results are parameter-free once we insist on approximate crossing symmetry for unitarized scattering amplitudes. We find that chiral symmetry predicts the existence of the axial-vector meson resonances ( $h_1(1170)$ ,  $h_1(1380)$ ,  $f_1(1285)$ ,  $a_1(1260)$ ,  $b_1(1235)$ ,  $K_1(1270)$ ,  $K_1(1400)$ ). A result analogous to the baryon sector [1, 13, 14] is found: in the heavy SU(3) limit with  $m_{\pi,K,\eta} \simeq 500$  MeV and  $m_{\rho,\omega,K^*,\phi} \simeq 900$  MeV the resonance states turn into bound states forming two degenerate octets and one singlet of the SU(3) flavor group with masses 1360 MeV and 1280 MeV respectively. Taking the light SU(3) limit with  $m_{\pi,K,\eta} \simeq 140$  MeV and  $m_{\rho,\omega,K^*,\phi} \simeq 700$  MeV we do not observe any bound-state nor resonance signals anymore. Since the leading order interaction kernel scales with  $N_c^{-1}$  the resonances disappear also in the large- $N_c$  limit. Using physical masses a pattern arises that compares surprisingly well with the empirical properties of the  $J^P = 1^-$  meson resonances.

## 2 The $\chi$ -BS(3) approach

The starting point to study the scattering of Goldstone bosons off vector mesons is the chiral SU(3) Lagrangian. The leading order Weinberg-Tomozawa

interaction Lagrangian density [15]

$$\mathcal{L}_{WT}(x) = -\frac{1}{16 f^2} \text{tr} \left( [\Phi^\mu(x), (\partial^\nu \Phi_\mu(x))]_- [\phi(x), (\partial_\nu \phi(x))]_- \right), \quad (1)$$

describes the s-wave interaction of the Goldstone bosons field  $\phi$  with a massive vector-meson field  $\Phi_\mu$ . The parameter  $f \simeq 90$  MeV in (1) is known from the weak decay process of the pions. In (1) we omit additional terms that do not contribute to the on-shell scattering amplitude of Goldstone bosons off vector-meson at tree-level.

As was emphasized in [1] the chiral SU(3) Lagrangian should not be used in perturbation theory except at energies sufficiently below all thresholds. Though the infinite set of irreducible diagrams can be successfully approximated by the standard perturbative chiral expansion that is no longer true for the infinite set of reducible diagrams once the energies are sufficiently large to support hadronic scattering processes. From an effective field theory point of view it is mandatory to sum the reducible diagrams. This is naturally achieved by considering the Bethe-Salpeter scattering equation. Since the intermediate vector mesons have in part a substantial decay width we allow for spectral distributions of the broadest vector mesons, the  $\rho_\mu$ - and  $K_\mu$ -mesons. In channels involving the  $\rho_\mu$ - or  $K_\mu$ -meson the two-particle propagator is folded with spectral functions obtained at the one-loop level describing the decay processes  $\rho_\mu \rightarrow \pi \pi$  and  $K_\mu \rightarrow \pi K$ .

The Bethe-Salpeter interaction kernel  $K_{\mu\nu}(\bar{k}, k; w)$  is the sum of all two-particle irreducible diagrams. The scattering problem decouples into thirteen orthogonal channels specified by isospin ( $I$ ), G-parity ( $G$ ) and strangeness ( $S$ ) quantum numbers. From a field theoretic point of view once the interaction kernel,  $K_{\mu\nu}(\bar{k}, k; w)$ , and the two-particle propagator,  $G$ , are specified the Bethe-Salpeter equation determines the scattering amplitude  $T_{\mu\nu}(\bar{k}, k; w)$ . However, in order to arrive at a scattering amplitude that does not depend on the choice of interpolating fields at given order in a truncation of the scattering kernel it is necessary to perform an on-shell reduction.

Progress is made in [2] by introducing an on-shell equivalent effective interaction kernel  $V$ , together with three off-shell interaction kernels  $V_L, V_R$  and  $V_{LR}$  where  $V_R$  ( $V_L$ ) vanishes if the initial (final) particles are on-shell. The interaction kernel  $V_{LR}$  is defined to vanish if evaluated with either initial or final particles on-shell. The latter objects are defined by:

$$\begin{aligned} K &= V + (1 - V \cdot G) \cdot V_L + V_R \cdot (1 - G \cdot V) \\ &+ (1 - V \cdot G) \cdot V_{LR} \cdot (1 - G \cdot V) - V_R \cdot \frac{1}{1 - G \cdot V_{LR}} \cdot G \cdot V_L. \end{aligned} \quad (2)$$

The decomposition of the Bethe-Salpeter interaction kernel is unique and can be applied to an arbitrary interaction kernel once it is defined what is meant with the 'on-shell' part of any two-particle amplitude. The latter we define as the part of the amplitude that has a decomposition into the complete set of projectors

$$V_{\mu\nu}(\bar{k}, k; w) = \sum_{J,P,a,b} V_{ab}^{(JP)}(\sqrt{s}) \mathcal{Y}_{\mu\nu,ab}^{(JP)}(\bar{q}, q; w), \quad (3)$$

where the projectors carry good total angular momentum  $J$  and parity  $P$ . It is clear that performing a chiral expansion of  $K$  and  $V$  to some order  $Q^n$  leads to a straight forward identification of the off-shell kernels  $V_L, V_R$  and  $V_{LR}$  to the same accuracy.

## 2.1 Renormalization scheme and crossing symmetry

Unlike in standard chiral perturbation theory the renormalization of a unitarized chiral perturbation theory is non-trivial and therefore requires particular care. The coefficient functions  $V_{ab}^{(JP)}(\sqrt{s})$  introduced in (3) are evaluated in chiral perturbation theory and therefore standard renormalization schemes are applicable. The on-shell part of the scattering amplitude takes the simple form,

$$T_{\mu\nu}^{\text{on-shell}}(\bar{k}, k; w) = \sum_{J,P} M^{(JP)}(\sqrt{s}) \mathcal{Y}_{\mu\nu}^{(JP)}(\bar{q}, q; w),$$

$$M^{(JP)}(\sqrt{s}) = \left[ 1 - V^{(JP)}(\sqrt{s}) J^{(JP)}(\sqrt{s}) \right]^{-1} V^{(JP)}(\sqrt{s}), \quad (4)$$

with a set of divergent loop functions  $J^{(JP)}(\sqrt{s})$ . The crucial issue is how to renormalize the loop functions. In [1] it was suggested to introduce a physical scheme defined by the renormalization condition,

$$T_{\mu\nu}^{(JP)}(\bar{k}, k; w) \Big|_{\sqrt{s}=\mu} = V_{\mu\nu}^{(JP)}(\bar{k}, k; w) \Big|_{\sqrt{s}=\mu}, \quad (5)$$

where the subtraction scale  $\mu = \mu(I, S)$  depends weakly on isospin and strangeness but is independent on  $J^P$ . It was argued in [1] that the optimal choice of the subtraction point can be determined by the requirement that the scattering amplitude is approximatively crossing symmetric. For the optimal subtraction scales  $\mu(I, S)$  we obtained,

$$\mu(I, 0) = M_{\rho(770)}, \quad \mu(I, \pm 1) = M_{K(892)}, \quad \mu(I, \pm 2) = M_{\rho(770)}. \quad (6)$$

Moreover it was demonstrated that the renormalization condition (5) is complete, i.e. the condition (5) suffices to render the scattering amplitude finite.

Before discussing in some detail the choice of the subtraction points  $\mu(I, S)$  let us elaborate on the structure of the loop functions. The merit of our scheme is that dimensional regularization can be used to evaluate the latter ones. Here we exploit the result that any given projector is a finite polynomial in the available 4-momenta. This implies that the loop functions can be expressed in terms of a log-divergent master function,  $I(\sqrt{s})$ , and reduced tadpole terms,

$$\begin{aligned}
J^{(JP)}(\sqrt{s}) &= N^{(JP)}(\sqrt{s}) \left( I(\sqrt{s}) - I(\mu) \right), \\
I(\sqrt{s}) &= \frac{1}{16\pi^2} \left( \frac{p_{cm}}{\sqrt{s}} \left( \ln \left( 1 - \frac{s - 2p_{cm}\sqrt{s}}{m^2 + M^2} \right) - \ln \left( 1 - \frac{s + 2p_{cm}\sqrt{s}}{m^2 + M^2} \right) \right) \right. \\
&\quad \left. + \left( \frac{1}{2} \frac{m^2 + M^2}{m^2 - M^2} - \frac{m^2 - M^2}{2s} \right) \ln \left( \frac{m^2}{M^2} + 1 \right) + I(0) \right), \quad (7)
\end{aligned}$$

where  $\sqrt{s} = \sqrt{M^2 + p_{cm}^2} + \sqrt{m^2 + p_{cm}^2}$ . The normalization factor  $N_a^{(JP)}(\sqrt{s})$  is a polynomial in  $\sqrt{s}$  and the mass parameters. In (7) the renormalization scale dependence of the scalar loop function  $I(\sqrt{s})$  was traded in favor of a dependence on a subtraction point  $\mu$ . The loop functions  $J^{(JP)}(\sqrt{s})$  are consistent with chiral counting rules only if the subtraction scale  $\mu \simeq M$  is chosen close to the 'heavy' meson mass [16, 1]. Moreover it was shown that keeping reduced tadpole terms in the loop functions leads to a renormalization of s-channel exchange terms that is in conflict with chiral counting rules. We emphasize that the projectors have the important property that in the case of broad intermediate states the implied loop functions follow from (7) by a simple folding with the spectral distributions of the two intermediate states.

The renormalization condition (5) reflects the basic assumption our effective field theory is built on, namely, that at subthreshold energies the scattering amplitudes may be evaluated in standard chiral perturbation theory. Once the available energy is sufficiently high to permit elastic two-body scattering a further typical dimensionless parameter of order one that is uniquely linked to the presence of a two-particle unitarity cut arise. Thus it is sufficient to sum those contributions keeping the perturbative expansion of all terms that do not develop a two-particle unitarity cut. In order to recover the perturbative nature of the subthreshold scattering amplitude the subtraction scale  $M - m < \mu < M + m$  must be chosen in between the s- and u-channel elastic unitarity branch points [1]. It was suggested that s-channel and u-channel unitarized amplitudes should be glued together at subthreshold kinematics [1]. A smooth result is guaranteed if the full amplitudes match the interaction kernel  $V$  close to the subtraction scale  $\mu$  as imposed by (5). In this case the crossing

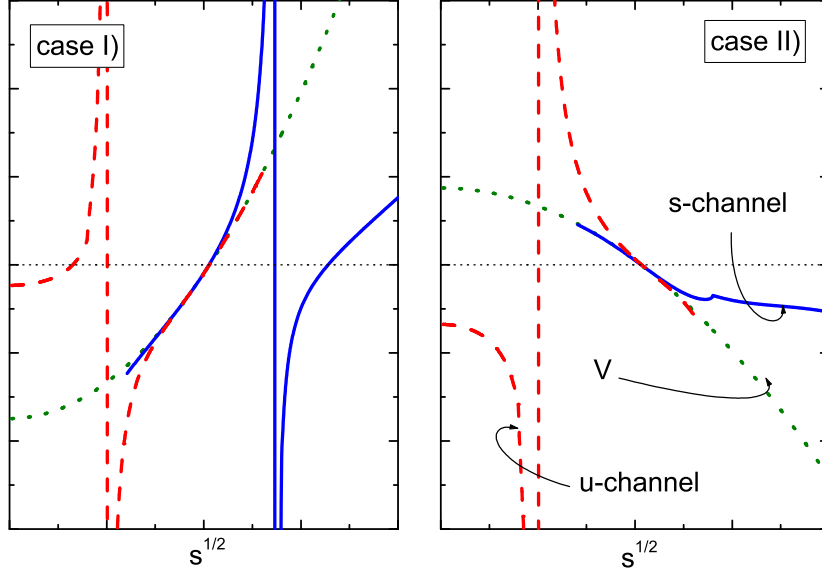


Figure 1: Typical cases of forward scattering amplitudes. The solid (dashed) line shows the s-channel (u-channel) unitarized scattering amplitude. The dotted lines represent the amplitude evaluated at tree-level.

symmetry of the interaction kernel, which follows directly from its perturbative evaluation, carries over to an approximate crossing symmetry of the full scattering amplitude. This construction reflects our basic assumption that diagrams showing an s-channel or u-channel unitarity cut need to be summed to all orders typically at energies where the diagrams develop their imaginary part. In Fig. 1 we demonstrate the quality of the proposed matching procedure as applied for typical forward scattering amplitudes. The figure clearly illustrates the smooth matching of s-channel and u-channel iterated amplitudes at subthreshold energies.

Given the subtraction scales as derived above the leading-order calculation is parameter-free. Of course chiral correction terms lead to further so far unknown parameters which need to be adjusted to data. Within the  $\chi$ -BS(3) approach such correction terms enter the effective interaction kernel  $V$  rather than leading to a change of the subtraction scales.

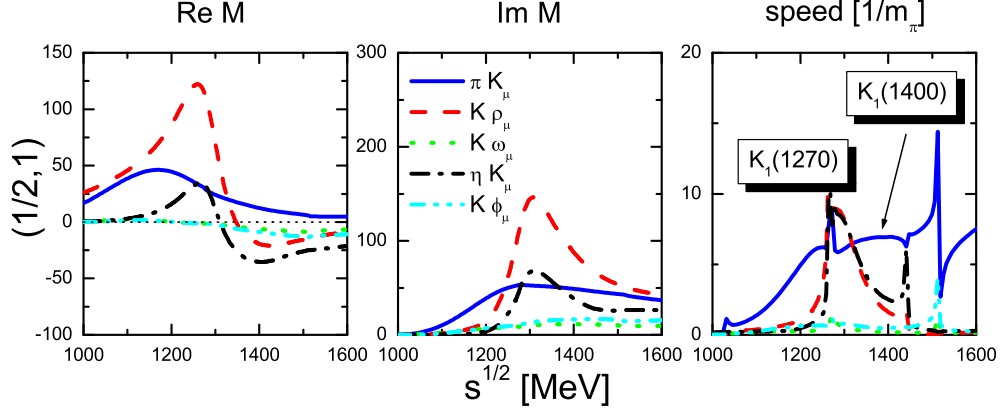


Figure 2: Scattering amplitudes and speeds for meson resonances with  $J^P = 1^+$  and  $(I, S) = (\frac{1}{2}, 1)$ .

### 3 Results

We present our results on s-wave scattering of Goldstone bosons off vector mesons using the leading order chiral SU(3) Lagrangian. Meson resonances with quantum number  $(I, S)$  and  $J^P = 1^+$  manifest themselves as poles in the corresponding scattering amplitudes  $M_{ab}^{JP}(\sqrt{s})$ .

To study the formation of meson resonances we generate speed plots (see [3]). The merit of producing speed plot lies in a convenient property of the latter allowing a straight forward extraction of resonance parameters. Assume that a coupled-channel amplitude  $M_{ab}(\sqrt{s})$  develops a pole of mass  $m_R$ , with

$$M_{ab}(\sqrt{s}) = -\frac{g_a^* g_b m_R}{\sqrt{s} - m_R + i\Gamma/2}, \quad \Gamma_a = \frac{|g_a|^2}{4\pi} |p_{cm}^{(a)}| N_a(m_R), \quad (8)$$

where the total resonance width,  $\Gamma$ , is given by the sum of all partial widths. The normalization factor  $N(M_R)$  in (8) is identical to the one entering the form of the loop functions in (7). The speed plots take a maximum at the resonance mass  $\sqrt{s} = m_R$ , with

$$\text{Speed}_{aa}(m_R) = \begin{cases} 2 \frac{\Gamma_a}{\Gamma^2} \left| 2 \sum_c \frac{\Gamma_c}{\Gamma} - 1 \right| & \text{if } a = \text{open} \\ 2 \frac{\Gamma_a}{\Gamma^2} \left| 2 \sum_c \frac{\Gamma_c}{\Gamma} - i \right| & \text{if } a = \text{closed}, \end{cases}$$

$$\Gamma = \sum_{a=\text{open}} \Gamma_a. \quad (9)$$

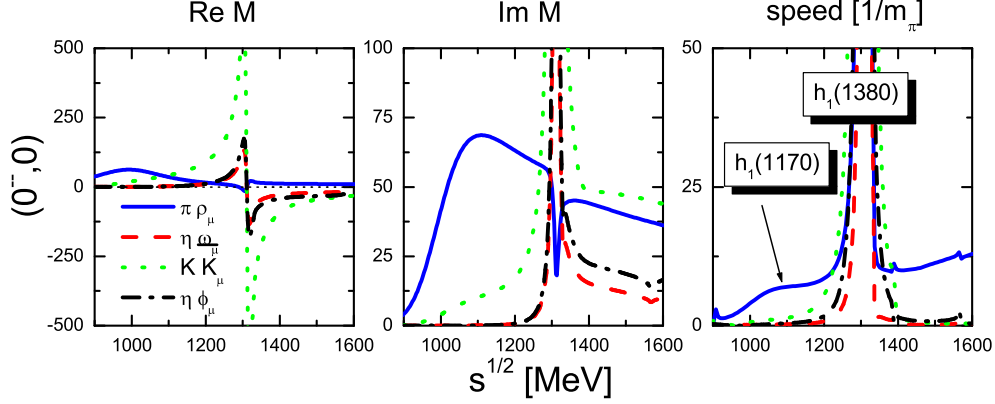


Figure 3: Scattering amplitudes and speeds for meson resonances with  $J^P = 1^+$  and  $(I^G, S) = (0^-, 0)$ .

The result (9) clearly demonstrates that the speed of a resonance in a given open channel  $a$  is not only a function of the total width parameter  $\Gamma$  and the partial width  $\Gamma_a$ . It does depend also on how strongly closed channels couple to that resonance. This is in contrast to the delay time of a resonance for which closed channels do not contribute.

To explore the multiplet structure of the resonance states we study first the 'heavy' SU(3) limit [13, 14] with  $m_{\pi, K, \eta} \simeq 500$  MeV and  $m_{\rho, \omega, K^*, \phi} \simeq 900$  MeV. In this case all resonance states turn into bound states forming two degenerate octets and one singlet of the SU(3) flavor group with masses 1367 MeV and 1289 MeV respectively. The latter numbers are quite insensitive to the precise value of the subtraction scale. For instance increasing (decreasing) the subtraction scale by 20 % away from its natural value the octet bound-state mass comes at 1383 MeV (1353 MeV). Our result is a direct reflection of the Weinberg-Tomozawa interaction,

$$8 \otimes 8 = 1 \oplus 8 \oplus 8 \oplus 10 \oplus \overline{10} \oplus 27, \quad (10)$$

which predicts attraction in the two octet and the singlet channel. This finding is analogous to the results of [13] that found two degenerate octet and one singlet state in the SU(3) limit of meson-baryon scattering with  $J^P = \frac{1}{2}^-$ . Taking the 'light' SU(3) limit [14] with  $m_{\pi, K, \eta} \simeq 140$  MeV and  $m_{\rho, \omega, K^*, \phi} \simeq 700$  MeV we do not observe any bound-state nor resonance signals anymore. A further interesting limit to study is  $N_c \rightarrow \infty$ . Since the scattering kernel is

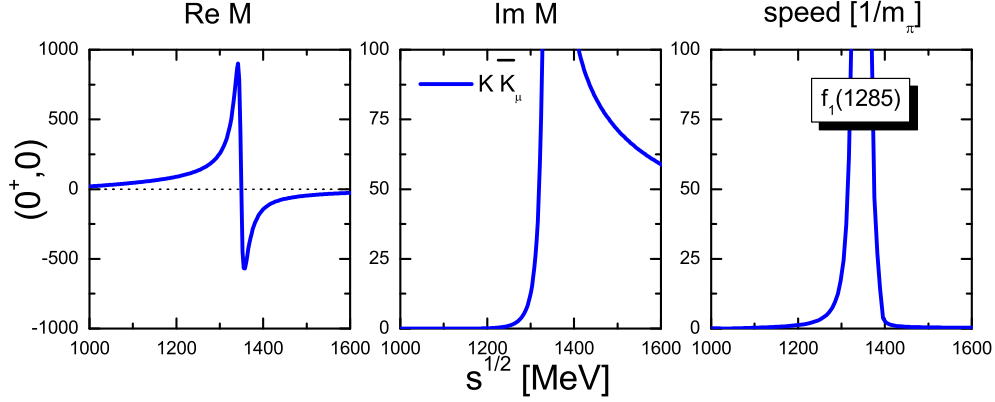


Figure 4: Scattering amplitudes and speeds for meson resonances with  $J^P = 1^+$  and  $(I^G, S) = (0^+, 0)$ .

proportional to the  $f^{-2} \sim N_c^{-1}$  the interaction strength vanishes in that limit and no resonances are generated.

Figs. 2-6 show the resonance spectrum that arises using physical masses using realistic spectral distributions for the broad vector mesons. The figures show real and imaginary parts of the scattering amplitudes as well as the associated speed plots. Clear signals in the speed plots of the  $(\frac{1}{2}, \pm 1)$ ,  $(0^\pm, 0)$  and  $(1^\pm, 0)$  channels are seen. No resonance is found in the remaining channels. The resonances can be unambiguously identified with the axial-vector meson resonances ( $h_1(1170)$ ,  $h_1(1380)$ ,  $f_1(1285)$ ,  $a_1(1260)$ ,  $b_1(1235)$ ,  $K_1(1270)$ ,  $K_1(1400)$ ).

In the 'heavy' SU(3) limit the  $(\frac{1}{2}, \pm 1)$  channel shows two bound states reflecting the presence of two degenerate octet states. Using physical masses the degeneracy is lifted and a narrow state at 1263 MeV and a broad state at about 1300 MeV arise. The effect of using realistic spectral distributions for the intermediate  $\rho_\mu$ - and  $K_\mu$ -mesons is demonstrated in Fig. 2. The resonance signal in the speed plots becomes much clearer since using spectral distributions for the broad intermediate states smears away the square-root singularities in the speeds at the corresponding thresholds. Our result is quite consistent with the empirical properties of the  $K_1(1270)$  meson. It has a width of about 90 MeV and decays dominantly into the  $K \rho_\mu$ -channel [17]. The second much broader state is assigned a width of about 175 MeV resulting almost exclusively from its decay into the  $\pi K_\mu$ -channel [17].

Similarly, in the heavy SU(3) limit the  $(0^-, 0)$  channel shows two bound

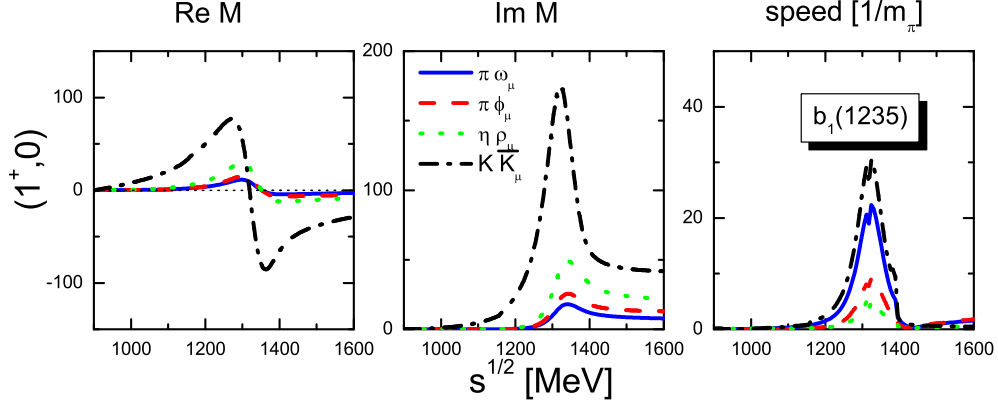


Figure 5: Scattering amplitudes and speeds for meson resonances with  $J^P = 1^+$  and  $(I^G, S) = (1^+, 0)$ .

states associated with a singlet and an octet state. Using physical masses a broad state at about 1100 MeV and a narrow state at 1303 MeV should be identified with the  $h_1(1170)$  and  $h_1(1380)$  resonance. Here we assign the  $h_1(1380)$ -resonance, for which its quantum numbers except its parity and angular momentum  $J^P = 1^+$  are unknown, the isospin and G-parity quantum numbers  $I^G = 0^-$ . This is a clear prediction of the chiral coupled-channel dynamics. The latter state has so far been seen only through its decay into the  $K \bar{K}_\mu$ - and  $\bar{K} K_\mu$ -channels [18]. Its small width of about 80 MeV [18] is consistent with the narrow structure seen in Fig. 3. The second resonances state in Fig. 3 is most clearly seen in the  $\pi\rho_\mu$ -channel. This is consistent with the empirical properties of the  $h_1(1170)$  resonance which so far has been seen only through its  $\pi\rho_\mu$ -decay leading to a large width of about 360 MeV [17].

The  $(0^+, 0)$ -speed (see Fig. 4) shows a bound-state at mass 1341 MeV a value somewhat above the mass of the  $f_1(1285)$  resonance. Using a spectral distribution for the  $K_\mu(892)$  in the intermediate states  $K \bar{K}_\mu$  and  $\bar{K} K_\mu$  states a narrow resonance appears. Its width of about 10 MeV is a factor two smaller than the empirical value [17]. The  $(1^+, 0)$ -speed of Fig. 5 shows a resonance at 1310 MeV to be identified with the  $b_1(1235)$  resonance. From the maximum of the imaginary part of the scattering amplitudes at the resonance peak one can directly read off ratios of coupling constants. Fig. 5 clearly demonstrates that the smallest coupling constant is predicted for the  $\pi\omega_\mu$ -channel. Nevertheless, the hadronic decay of the  $b_1(1235)$  is completely dominated by the

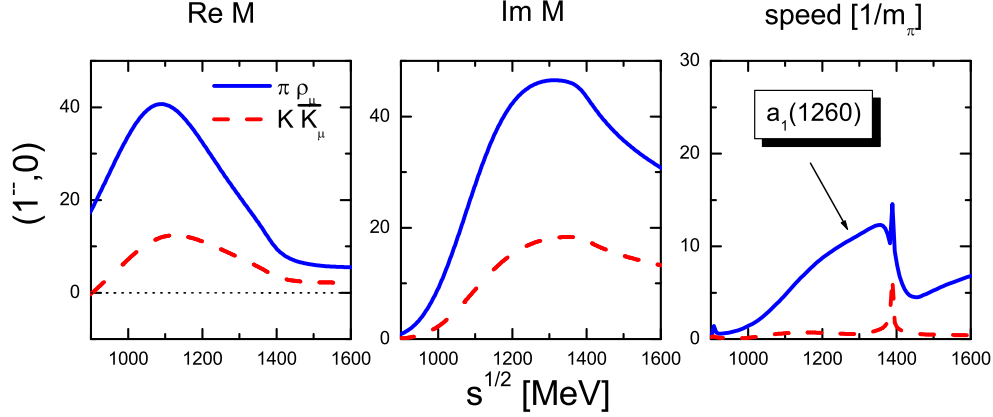


Figure 6: Scattering amplitudes and speeds for meson resonances with  $J^P = 1^+$  and  $(I^G, S) = (1^-, 0)$ .

$\pi\omega_\mu$ -channel. This is a simple consequence of phase-space kinematics. The widths of the resonance as indicated by Fig. 5 is quite compatible with the empirical value of about 140 MeV [17]. The  $a_1(1260)$  resonance is found in the  $(1^-, 0)$ -speed of Fig. 3 as a broad peak with a mass of about 1300 MeV. Empirically its width is estimated to be about 250-600 MeV [17] resulting from its decay into the  $\pi\rho$ -channel.

The structure of the  $h_1(1380)$ ,  $f_1(1285)$  and  $b_1(1235)$  resonances as predicted by chiral coupled-channel dynamics is quite intriguing since those resonances couple dominantly to the  $K\bar{K}_\mu$ -channel. This implies that the latter channel is the driving force that generates these resonances dynamically. This finding is very much analogous to the structure of the scalar  $f_0(980)$  resonance that strongly couples to the  $K\bar{K}$ -channel and emphasizes the importance of the chiral SU(3) symmetry even for non-strange resonances. It should be emphasized that the results obtained here at leading order can be improved further by incorporating chiral correction terms into the analysis. In view of the remarkable success of the leading order Weinberg-Tomozawa interaction one would expect a rapidly converging expansion.

## References

- [1] M.F.M. Lutz and E. E. Kolomeitsev, Nucl. Phys. A **700** (2002) 193.
- [2] M.F.M. Lutz, GSI-Habil-2002-1.
- [3] M.F.M. Lutz and E. E. Kolomeitsev, Nucl. Phys. A **730** (2004) 392.
- [4] N.A Törnqvist, Phys. Rev. Lett. **49** (1982) 624.
- [5] E. van Beveren et al., Z. Phys. C **30** (1986) 615.
- [6] J. Nieves, M.P. Valderrama and E. Ruiz Arriola, Phys. Rev. D **65** (2002) 036002.
- [7] A.G. Nicola and J.R. Pelaez, Phys. Rev. D **65** (2002) 054009.
- [8] H.W. Wyld, Phys. Rev. **155** (1967) 1649.
- [9] R.H. Dalitz, T.C. Wong and G. Rajasekaran, Phys. Rev. **153** (1967) 1617.
- [10] J.S. Ball and W.R. Frazer, Phys. Rev. Lett. **7** (1961) 204.
- [11] G. Rajasekaran, Phys. Rev. **5** (1972) 610.
- [12] R.K. Logan and H.W. Wyld, Phys. Rev. **158** (1967) 1467.
- [13] C. García-Recio, M.F.M. Lutz and J. Nieves, Phys. Lett. B **582** (2004) 49.
- [14] E.E. Kolomeitsev and M.F.M. Lutz, Phys. Lett. B in print, nucl-th/0305101.
- [15] S. Weinberg, Phys. Rev. Lett. **17** (1966) 616; Y. Tomozawa, Nuov. Cim. A **46** (1966) 707.
- [16] M.F.M. Lutz and E. E. Kolomeitsev, Proc. of Int. Workshop XXVIII on Gross Properties of Nuclei and Nuclear Excitations, Hirschegg, Austria, January 16-22, 2000, nucl-th/0004021.
- [17] K. Hagiwara et al., Phys. Rev. D **66** (2002) 010001.
- [18] Particle Data Group, Eur. Phys. J. C **15** (2000) 1.